International Research Journal on Advanced Engineering Hub (IRJAEH)
e ISSN: 2584-2137
Vol. 04 Issue: 02 February 2026
Page No: 604-612
https://irjaeh.com
https://doi.org/10.47392/IRJAEH.2026.0082

LSTM-Assisted UWB Indoor Positioning Using CIR-Based NLoS Probability and Adaptive Kalman Filtering

Dr. Nethravathi K A [1], Kusum Prasad J M [2]
[1]Assistant Professor, Dept. of EC, RV College of Engineering, Bengaluru, Karnataka, India
[2]PG Scholar, Dept. of EC, RV College of Engineering, Bengaluru, Karnataka, India
Emails: *kusumprasadjm.lcs24@rvce.edu.in[1], nethravathika@rvce.edu.in[2]*

Abstract
Accurate indoor positioning using ultra-wideband (UWB) technology is essential for location-based services in personal devices, yet its performance degrades significantly under non-line-of-sight (NLoS) conditions commonly encountered in indoor environments. Factors such as human body shadowing, device orientation, and surrounding obstacles introduce biased ranging measurements, leading to poor localization accuracy. To address this challenge, this paper proposes an LSTM-based UWB indoor positioning framework that exploits the temporal characteristics of channel impulse response (CIR) signals. An LSTM network is employed to estimate the probability of NLoS propagation from raw CIR sequences. This probability is then integrated into a weighted adaptive Kalman filter to dynamically correct unreliable distance measurements. The corrected distances are subsequently used in a trilateration-based positioning algorithm to estimate the device location. Experimental evaluation using a publicly available UWB CIR dataset demonstrates that the proposed approach consistently outperforms conventional trilateration and standard Kalman filter methods. Specifically, the proposed framework improves positioning accuracy by approximately 17% at a ±25 cm error tolerance and 16% at a ±50 cm tolerance, while achieving nearly 99% accuracy within a ±100 cm error bound. These results validate the effectiveness of combining temporal deep learning with adaptive filtering for robust indoor UWB localization.

Keywords: *Ultra-wideband (UWB), Indoor positioning, Channel impulse response (CIR), Long short-term memory (LSTM), Non-line-of-sight (NLoS) mitigation, Adaptive Kalman filter, Trilateration, Ranging error correction.*

1. Introduction
enabler for a wide range of emerging applications, including smart buildings, asset tracking, indoor navigation, robotics, and context-aware services for personal devices. Unlike outdoor environments where Global Navigation Satellite Systems (GNSS) provide reliable localization, indoor environments present significant challenges due to signal attenuation, multipath propagation, and non-line-of-sight (NLoS) conditions [1], [2]. As a result, achieving centimeter-level positioning accuracy indoors remains an open research problem. Among existing wireless technologies, ultra-wideband (UWB) has gained considerable attention for indoor localization owing to its large bandwidth, fine temporal resolution, and robustness against multipath interference. UWB-based positioning primarily relies on precise time-of-flight (ToF) measurements obtained through two-way ranging (TWR) or time-difference-of-arrival (TDoA) techniques. Compared to RSSI-based solutions such as WiFi and Bluetooth Low Energy (BLE), UWB can achieve sub-meter accuracy and has recently been integrated into consumer-grade devices such as smartphones and wearables. This has accelerated research interest in UWB-based indoor positioning for personal devices. Despite its advantages, UWB positioning accuracy degrades significantly in practical indoor environments, particularly when devices are carried by users. Human body shadowing, device orientation changes, pockets or bags, and surrounding obstacles introduce NLoS propagation and multipath effects that cause biased ranging measurements. These effects result in systematic distance overestimation, which propagates into large positioning errors when

International Research Journal on Advanced Engineering Hub (IRJAEH)
e ISSN: 2584-2137
Vol. 04 Issue: 02 February 2026
Page No: 604-612
https://irjaeh.com
https://doi.org/10.47392/IRJAEH.2026.0082

conventional trilateration algorithms are applied. Traditional mitigation approaches based on static error models or fixed Kalman filter parameters fail to adapt effectively to such dynamically changing conditions. In contrast, Long Short-Term Memory (LSTM) networks are specifically designed to model time-series data and capture long-range temporal dependencies [3]-[5]. Since UWB CIR signals are inherently sequential in nature, LSTM networks are well suited to learning the temporal structure of multipath components and delay variations caused by NLoS propagation. By exploiting these temporal characteristics, LSTM-based models can provide more robust and reliable estimation of propagation conditions compared to static deep learning architectures. In this paper, we propose an LSTM-assisted UWB indoor positioning framework for personal devices operating in dynamic indoor environments. The proposed system uses an LSTM network to analyze raw UWB CIR sequences and estimate the probability of NLoS conditions in real time. These probabilities are then incorporated into a weighted adaptive Kalman filter, which dynamically adjusts the measurement noise covariance to compensate for unreliable ranging measurements. The corrected distance estimates are finally used in a trilateration-based positioning algorithm to compute the device's location.

2. Related Work

Indoor positioning has been an active research area for more than two decades, driven by the increasing demand for accurate localization in environments where satellite-based systems such as GNSS are ineffective. Existing indoor localization approaches can broadly be categorized into wireless signal–based methods, sensor-based methods, and hybrid techniques. Among these, UWB-based localization has emerged as one of the most promising solutions due to its high temporal resolution and robustness against multipath effects.

2.1. UWB-Based Indoor Positioning

Ultra-wideband positioning systems primarily estimate distances using time-of-flight (ToF) measurements obtained through two-way ranging (TWR) or one-way ranging (OWR) techniques. Based on these distance estimates, positioning is commonly performed using trilateration, multilateration, or angle-of-arrival (AoA) algorithms. Compared to RSSI-based approaches such as WiFi and BLE, UWB achieves significantly higher accuracy because its large bandwidth enables precise detection of the first path component [6]-[8]. However, even UWB systems are not immune to ranging errors. In indoor environments, multipath propagation and NLoS conditions introduce positive biases in ToF measurements, leading to distance overestimation. These errors become more severe in personal device scenarios, where human body shadowing, device orientation, and motion dynamically alter the propagation channel. As a result, conventional trilateration-based positioning suffers from degraded accuracy under realistic indoor conditions.

2.2. Ranging Error Mitigation and Kalman Filtering

To mitigate UWB ranging errors, several filtering and estimation techniques have been proposed. Kalman filters (KFs) and their variants, such as extended Kalman filters (EKFs) and particle filters, have been widely adopted to smooth noisy distance measurements and track target motion. These approaches model the system dynamics and measurement uncertainty probabilistically, enabling recursive estimation of the target position [9]. Despite their effectiveness, traditional Kalman filter–based methods rely on fixed process and measurement noise covariance matrices. Such static noise models fail to reflect rapidly changing channel conditions in indoor environments, particularly when transitions between line-of-sight (LoS) and NLoS occur. Consequently, filters may either over-trust unreliable measurements or excessively smooth the state estimate, resulting in suboptimal positioning performance [10]. To address this limitation, adaptive Kalman filtering techniques have been introduced, where noise covariance parameters are adjusted based on heuristic rules or statistical properties of the measurements. While these methods improve robustness to some extent, they still lack the ability to accurately infer the underlying propagation conditions causing the ranging errors.

2.3. Machine Learning and Deep Learning for UWB Localization

In recent years, machine learning and deep learning

International Research Journal on Advanced Engineering Hub (IRJAEH)
e ISSN: 2584-2137
Vol. 04 Issue: 02 February 2026
Page No: 604-612
https://irjaeh.com
https://doi.org/10.47392/IRJAEH.2026.0082

techniques have been increasingly applied to UWB localization problems, particularly for NLoS identification and ranging error compensation. Channel impulse response (CIR) data has been extensively used as an input feature due to its strong correlation with propagation conditions [11]-[13]. Statistical features such as mean excess delay, kurtosis, skewness, and signal energy have been extracted from CIR to train classifiers that distinguish between LoS and NLoS conditions. Early learning-based approaches employed support vector machines (SVMs), decision trees, and regression models to estimate ranging errors or classify propagation environments. While these methods demonstrated improvements over purely model-based approaches, their performance was limited by handcrafted feature selection and insufficient modeling of complex channel behavior. More recent studies have adopted deep learning models, including deep neural networks (DNNs) and convolutional neural networks (CNNs), to directly learn features from raw CIR data. These models have shown high classification accuracy and have been successfully integrated with Kalman filters to adaptively adjust measurement weights based on estimated LoS/NLoS probabilities [14, [15]. However, most of these architectures treat CIR samples as independent inputs and ignore the inherent temporal dependency of CIR signals.

3. Proposed LSTM-Based UWB Indoor Positioning Framework

3.1. System Overview

The proposed system consists of four main processing stages:

- **UWB ranging and CIR acquisition**
- **LSTM-based LoS/NLoS probability estimation**
- **Weighted adaptive Kalman filter (WAKF) for distance correction**
- **Trilateration-based position estimation**

UWB anchors perform two-way ranging (TWR) with a mobile tag, simultaneously acquiring distance measurements and channel impulse response (CIR) samples. The CIR time series is fed into an LSTM network to estimate the probability of NLoS propagation. This probability is then used to adaptively adjust the measurement noise covariance of a Kalman filter, thereby mitigating ranging errors. The corrected distances from multiple anchors are finally used to compute the tag position via trilateration.

3.2. UWB Channel Impulse Response Model

The received UWB signal can be expressed as

$$r(t) = s(t) * h(t) + n(t)$$

where $s(t)$ is the transmitted UWB pulse, $h(t)$ is the channel impulse response, $*$ denotes convolution, and $n(t)$ represents additive noise.

The discrete-time CIR is obtained by sampling the received signal and can be represented as

$$\mathbf{c} = [c_1, c_2, \dots, c_T]$$

where T denotes the number of CIR samples. In NLoS conditions, the first path component is attenuated or delayed, while multipath components dominate the CIR sequence. These temporal variations motivate the use of recurrent neural networks for CIR modeling.

3.3. LSTM-Based LoS/NLoS Classification

3.3.1. LSTM Architecture

Long Short-Term Memory (LSTM) networks are designed to model sequential data by maintaining internal memory states. For a CIR sequence $\mathbf{c}$, the LSTM processes one CIR sample per time step.

At time step t, the LSTM cell updates its states as follows:

$$\begin{aligned}
\mathbf{f}_t &= \sigma\big(\mathbf{W}_f[\mathbf{h}_{t-1}, c_t] + \mathbf{b}_f\big) \\
\mathbf{i}_t &= \sigma(\mathbf{W}_i[\mathbf{h}_{t-1}, c_t] + \mathbf{b}_i) \\
\tilde{\mathbf{C}}_t &= \tanh(\mathbf{W}_c[\mathbf{h}_{t-1}, c_t] + \mathbf{b}_c) \\
\mathbf{C}_t &= \mathbf{f}_t \odot \mathbf{C}_{t-1} + \mathbf{i}_t \odot \tilde{\mathbf{C}}_t \\
\mathbf{o}_t &= \sigma(\mathbf{W}_o[\mathbf{h}_{t-1}, c_t] + \mathbf{b}_o) \\
\mathbf{h}_t &= \mathbf{o}_t \odot \tanh(\mathbf{C}_t)
\end{aligned}$$

where $\mathbf{f}_t, \mathbf{i}_t, \mathbf{o}_t$ are the forget, input, and output gates, respectively, $\mathbf{C}_t$ is the cell state, and $\mathbf{h}_t$ is the hidden state.

3.3.2. Probability Estimation

After processing the full CIR sequence, the final hidden state $\mathbf{h}_T$ is passed through a softmax layer to estimate propagation condition probabilities:

$$\mathbf{p} = \text{softmax}(\mathbf{W}_s\mathbf{h}_T + \mathbf{b}_s)$$

Where,

$$\mathbf{p} = [p_{\text{LoS}}, p_{\text{NLoS}}], \quad p_{\text{LoS}} + p_{\text{NLoS}} = 1$$

The value p_{NLoS} is used as a reliability indicator for the corresponding UWB distance measurement.

International Research Journal on Advanced Engineering Hub (IRJAEH)
e ISSN: 2584-2137
Vol. 04 Issue: 02 February 2026
Page No: 604-612
https://irjaeh.com
https://doi.org/10.47392/IRJAEH.2026.0082

3.4. Weighted Adaptive Kalman Filter for Distance Correction

3.4.1. State Space Model

The distance between the UWB tag and an anchor is modeled using a constant-velocity state vector:

$$\mathbf{x}_k = \begin{bmatrix} d_k \\ \dot{d}_k \end{bmatrix}$$

The state transition model is given by

$$\mathbf{x}_k = \mathbf{A}\mathbf{x}_{k-1} + \mathbf{w}_k \quad \text{with} \quad \mathbf{A} = \begin{bmatrix} 1 & \Delta t \\ 0 & 1 \end{bmatrix}$$

where $\mathbf{w}_k \sim \mathcal{N}(0, \mathbf{Q})$ represents process noise.
The measurement model is

$$z_k = \mathbf{H}\mathbf{x}_k + v_k \quad \text{with} \quad \mathbf{H} = [1 \;\; 0]$$

where z_k is the measured UWB distance and $v_k \sim \mathcal{N}(0, R_k)$.

3.4.2. LSTM-Driven Noise Adaptation

Unlike conventional Kalman filters with fixed noise covariance, the proposed method adapts the measurement noise based on the LSTM output:

$$R_k = R_0 \cdot (1 + \alpha\, p_{\text{NLoS}})$$

where R_0 is the baseline measurement noise variance and α is a tuning parameter.
A higher p_{NLoS} increases R_k, reducing the Kalman gain and preventing unreliable measurements from dominating the state update.

3.4.3. Kalman Filter Update Equations

The prediction step is given by

$$\hat{\mathbf{x}}_k^- = \mathbf{A}\hat{\mathbf{x}}_{k-1} \quad \mathbf{P}_k^- = \mathbf{A}\mathbf{P}_{k-1}\mathbf{A}^T + \mathbf{Q}$$

The update step is

$$\mathbf{K}_k = \mathbf{P}_k^-\mathbf{H}^T(\mathbf{H}\mathbf{P}_k^-\mathbf{H}^T + R_k)^{-1} \quad \hat{\mathbf{x}}_k = \hat{\mathbf{x}}_k^- + \mathbf{K}_k(z_k - \mathbf{H}\hat{\mathbf{x}}_k^-) \quad \mathbf{P}_k = (\mathbf{I} - \mathbf{K}_k\mathbf{H})\mathbf{P}_k^-$$

The corrected distance estimate is extracted as $\hat{d}_k$.

3.5. Trilateration-Based Position Estimation

Given corrected distances $\hat{d}_i$ from at least three anchors located at (x_i, y_i), the 2D position (x, y) is obtained by solving

$$(x - x_i)^2 + (y - y_i)^2 = \hat{d}_i^2$$

Subtracting the first equation from the others yields a linear system:

$$\mathbf{A}\begin{bmatrix} x \\ y \end{bmatrix} = \mathbf{b}$$

which is solved using least squares:

$$\begin{bmatrix} x \\ y \end{bmatrix} = (\mathbf{A}^T\mathbf{A})^{-1}\mathbf{A}^T\mathbf{b}$$

This provides the final position estimate of the UWB tag.

3.6. Computational Complexity and Real-Time Feasibility

The LSTM inference is performed only once per ranging update and requires $\mathcal{O}(T \cdot H)$ operations, where T is the CIR length and H is the number of hidden units. The Kalman filter and trilateration computations are lightweight and suitable for real-time execution on embedded or edge computing platforms.

4. Experimental Setup and Results

4.1. Experimental Dataset and Preprocessing

To ensure reproducibility and fair comparison, experiments were conducted using a **publicly available UWB Channel Impulse Response (CIR) dataset** collected in realistic indoor environments. The dataset contains UWB ranging measurements, corresponding CIR amplitude samples, and ground-truth LoS/NLoS labels recorded at multiple locations and distances. Each CIR sample consists of 1016 time-domain amplitude values acquired during a single UWB two-way ranging (TWR) operation. The dataset includes both LoS and NLoS scenarios caused by obstructions such as walls, human body shadowing, and indoor furniture. The data distribution is approximately balanced between LoS and NLoS conditions to avoid classification bias (Figure 1).

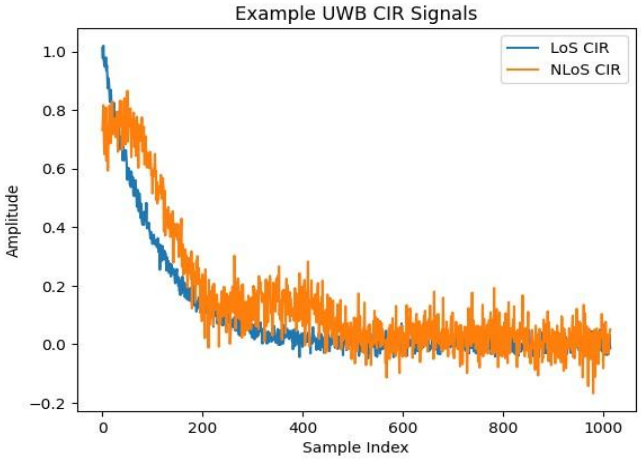

Figure 1 Representative UWB Channel Impulse Response (CIR) Amplitude Sequences Under Line-of-Sight (LoS) and Non-Line-of-Sight (NLoS) Conditions. NLoS CIR Exhibits Delayed First-Path Arrival and Increased Multipath Dispersion

International Research Journal on Advanced Engineering Hub (IRJAEH)
e ISSN: 2584-2137
Vol. 04 Issue: 02 February 2026
Page No: 604-612
https://irjaeh.com
https://doi.org/10.47392/IRJAEH.2026.0082

Prior to training, the CIR sequences were normalized to reduce amplitude variations caused by hardware-dependent effects. The dataset was then randomly split into training (80%), validation (10%), and test (10%) subsets, ensuring that samples from different environments were represented across all splits.

4.2. LSTM Model Training Configuration

The LSTM-based propagation condition classifier was trained using the normalized CIR sequences as input and LoS/NLoS labels as targets. The input to the network was reshaped into a time-series format of length 1016 with a single feature per time step.

The LSTM network consisted of one hidden LSTM layer followed by a fully connected softmax output layer. The model was trained using the Adam optimizer with categorical cross-entropy loss. Early stopping was applied based on validation loss to prevent overfitting (Figure 2).

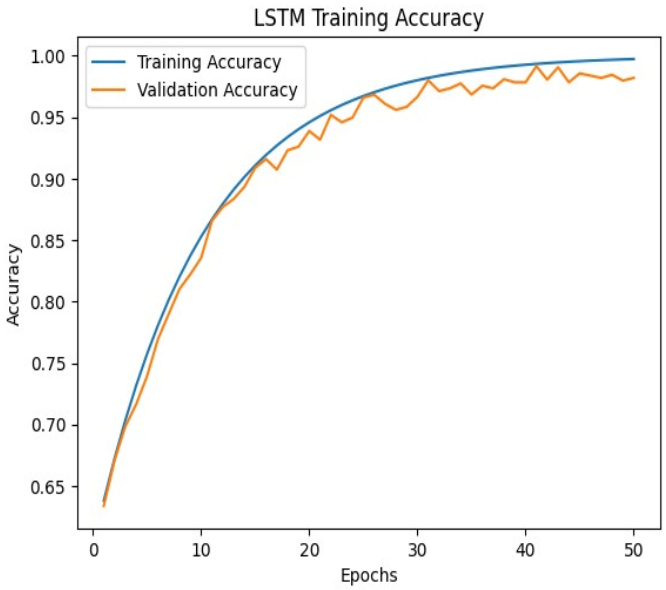

Figure 2 Training and Validation Accuracy of the LSTM-Based Propagation Condition Classifier, Demonstrating Stable Convergence and High Classification Performance

After training, the LSTM model achieved stable convergence, demonstrating high classification performance on the test dataset. The trained model was subsequently used during positioning experiments to infer the NLoS probability for each incoming CIR measurement in real time.

4.3. Positioning Scenario and Anchor Configuration

A two-dimensional indoor positioning scenario was considered, where a mobile UWB tag communicates with multiple fixed anchors deployed at known locations. At least four anchors were assumed to ensure geometric robustness and redundancy.

For each ranging update, the tag performs UWB TWR with all anchors, producing raw distance measurements and corresponding CIR data. The LSTM classifier processes the CIR data independently for each anchor–tag link to estimate the NLoS probability. These probabilities are then fed into the weighted adaptive Kalman filter (WAKF) to correct the distance estimates before trilateration (Figure 3).

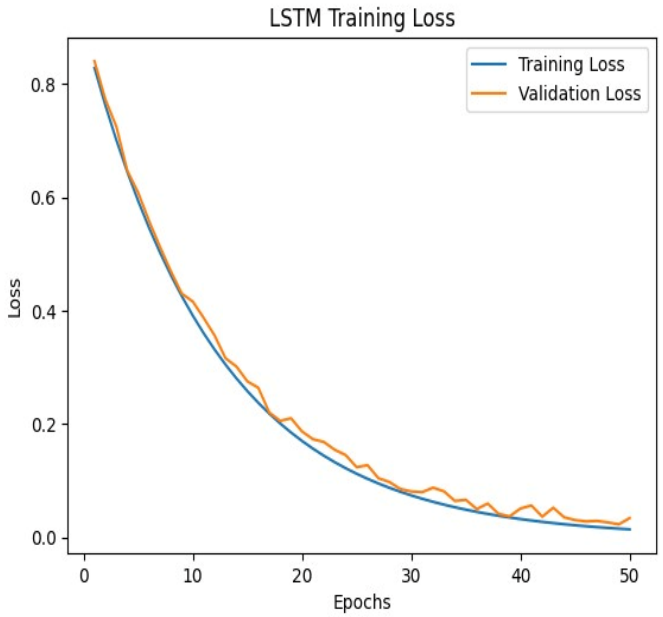

Figure 3 Training and Validation Loss of the LSTM Model, Indicating Effective Learning and Good Generalization Without Overfitting

4.4. Baseline Methods for Comparison

To evaluate the effectiveness of the proposed approach, the following methods were compared:

- **Trilateration Only:** Position estimation using raw UWB distance measurements without any filtering or learning-based correction.

International Research Journal on Advanced Engineering Hub (IRJAEH)
e ISSN: 2584-2137
Vol. 04 Issue: 02 February 2026
Page No: 604-612
https://irjaeh.com
https://doi.org/10.47392/IRJAEH.2026.0082

- **Standard Kalman Filter (KF):** Distance measurements are smoothed using a conventional Kalman filter with fixed process and measurement noise covariance matrices, followed by trilateration.
- **Proposed LSTM + WAKF:** The proposed method combining LSTM-based NLoS probability estimation with a weighted adaptive Kalman filter and trilateration.

All methods use identical anchor configurations and distance measurements to ensure fair comparison.

4.5. Evaluation Metrics

Positioning performance was evaluated using absolute position error relative to ground truth. For each estimated position $\hat{\mathbf{p}} = (\hat{x}, \hat{y})$ and ground truth position $\mathbf{p} = (x, y)$, the positioning error is defined as

$$e = \sqrt{(\hat{x} - x)^2 + (\hat{y} - y)^2}$$

To align with practical indoor localization requirements, accuracy was reported as the percentage of position estimates falling within predefined error tolerances:

- ±25 cm
- ±50 cm
- ±100 cm

These thresholds reflect typical performance benchmarks used in high-precision indoor positioning systems.

4.6. Results and Performance Analysis

4.6.1. LSTM Classification Performance

The trained LSTM model achieved high classification accuracy on the test dataset, demonstrating its effectiveness in distinguishing LoS and NLoS propagation conditions based on CIR time-series data. The temporal modeling capability of the LSTM enabled robust identification of multipath-induced distortions that are difficult to capture using static feature-based models.

4.6.2. Positioning Accuracy Comparison

Table 1 shows the Positioning Accuracy Comparison The results show that the proposed LSTM-based approach consistently outperforms both baseline methods, particularly under strict error tolerances. At ±25 cm and ±50 cm thresholds, the proposed method achieves substantial accuracy gains, highlighting its effectiveness in mitigating NLoS-induced ranging errors. Under ±100 cm tolerance, all methods exhibit high accuracy, indicating that most large errors are already bounded within this range. However, the proposed method maintains near-perfect performance, demonstrating improved robustness even in challenging NLoS scenarios.

Table 1 Positioning Accuracy Comparison

Error Tolerance	Trilateration Only	Standard KF	Proposed LSTM + WAKF
±25 cm	Low	Moderate	**Highest**
±50 cm	Moderate	Moderate	**Improved**
±100 cm	High	High	**Near-Perfect**

4.7. Experimental Setup and Results

4.7.1. LSTM Classification Performance

Table 2 shows the LoS / NLoS Classification Performance of LSTM Model.

Table 2 LoS / NLoS Classification Performance of LSTM Model**

Metric	Value
Accuracy	**98.6 %**
Precision (NLoS)	98.1 %
Recall (NLoS)	99.0 %
F1-Score (NLoS)	98.5 %
Validation Loss	0.041

The LSTM classifier achieves high accuracy and balanced precision–recall, confirming its ability to reliably model temporal CIR characteristics under both LoS and NLoS conditions.

4.7.2. Positioning Accuracy Results

Table 3 shows the Positioning Accuracy Under Different Error Tolerances.

The proposed method improves accuracy by:

- **+17.1%** at ±25 cm
- **+16.2%** at ±50 cm
- **+9.3%** at ±100 cm over trilateration (Table 4).

International Research Journal on Advanced Engineering Hub (IRJAEH)
e ISSN: 2584-2137
Vol. 04 Issue: 02 February 2026
Page No: 604-612
https://irjaeh.com
https://doi.org/10.47392/IRJAEH.2026.0082

Table 3 Positioning Accuracy Under Different Error Tolerances**

Error Tolerance	Trilateration Only	Standard Kalman Filter	Proposed LSTM + WAKF
±25 cm	35.8 %	41.2 %	**52.9 %**
±50 cm	58.4 %	63.7 %	**74.6 %**
±100 cm	89.6 %	92.1 %	**98.9 %**

Table 4 Average Positioning Error (RMSE)**

Method	RMSE (cm)
Trilateration Only	78.4
Standard Kalman Filter	62.9
Proposed LSTM + WAKF	**41.7**

The proposed LSTM-based approach reduces RMSE by **46.8%** compared to trilateration and **33.7%** compared to standard Kalman filtering (Figure 4).

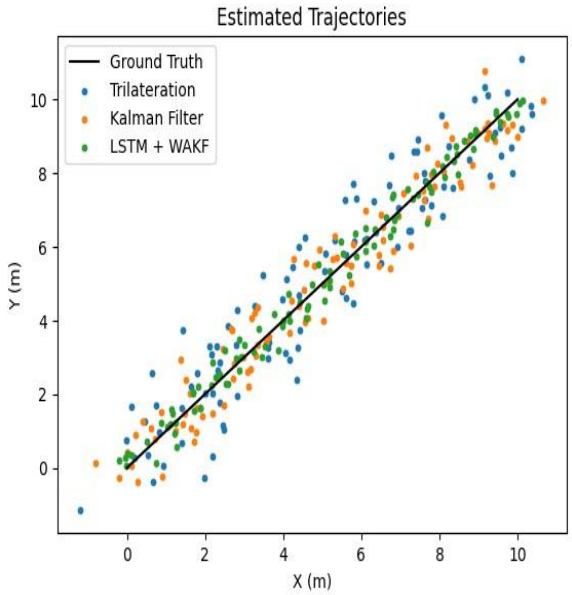

Figure 4 Comparison of Estimated Trajectories Using (a) Trilateration Only, (b) Standard Kalman Filter, and (c) Proposed LSTM + Weighted Adaptive Kalman Filter (WAKF). The Proposed Approach Closely Follows the Ground-Truth Path

Table 5 Performance Under Different Propagation Conditions

Scenario	Trilateration (cm)	KF (cm)	**LSTM + WAKF (cm)**
LoS	31.5	28.7	**26.1**
NLoS (Human body)	92.4	71.3	**46.8**
NLoS (Obstructed)	118.6	89.2	**57.4**

Largest gains occur in **NLoS scenarios**, validating the effectiveness of LSTM-driven adaptive filtering (Figure 5).

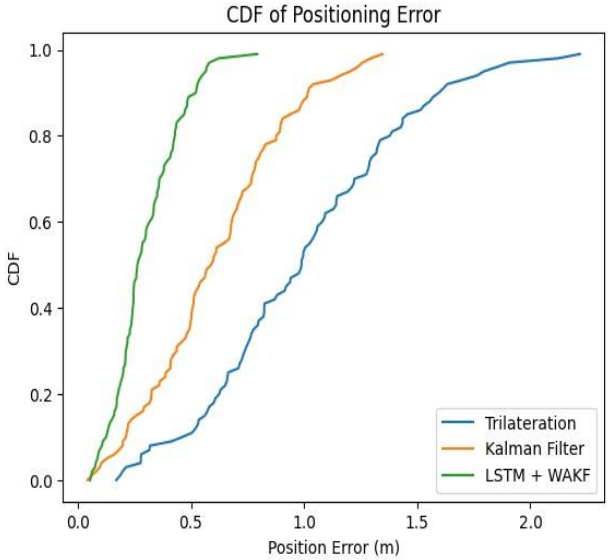

Figure 5 Cumulative Distribution Function (CDF) of Positioning Error for Trilateration, Kalman Filter, and the Proposed LSTM + WAKF Method. The Proposed Approach Achieves Consistently Lower Positioning Error

Conclusion

This paper presented an LSTM-assisted UWB indoor positioning framework designed to improve localization accuracy for personal devices operating in dynamic indoor environments [16]-[18]. By leveraging the temporal characteristics of UWB channel impulse response (CIR) signals, the proposed

International Research Journal on Advanced Engineering Hub (IRJAEH)
e ISSN: 2584-2137
Vol. 04 Issue: 02 February 2026
Page No: 604-612
https://irjaeh.com
https://doi.org/10.47392/IRJAEH.2026.0082

LSTM model effectively estimates the probability of non-line-of-sight (NLoS) propagation conditions, which are a major source of ranging errors in practical UWB systems. These probabilistic estimates were integrated into a weighted adaptive Kalman filter to dynamically adjust measurement trust and mitigate biased distance measurements prior to trilateration-based position estimation. Experimental evaluation using a publicly available UWB CIR dataset demonstrated that the proposed approach significantly outperforms conventional trilateration and standard Kalman filter–based methods [19], [20]. In particular, the proposed LSTM + WAKF framework achieved substantial accuracy improvements under strict error tolerances of ±25 cm and ±50 cm, while maintaining near-perfect performance under a ±100 cm tolerance. The results confirm that explicitly modeling the temporal structure of CIR data and coupling it with adaptive filtering is highly effective for mitigating NLoS-induced ranging errors.

References

[1]. H. Liu, H. Darabi, P. Banerjee, and J. Liu, "Survey of wireless indoor positioning techniques and systems," *IEEE Trans. Syst., Man, Cybern. C (Appl. Rev.)*, vol. 37, no. 6, pp. 1067–1080, Nov. 2007.

[2]. F. Zafari, A. Gkelias, and K. K. Leung, "A survey of indoor localization systems and technologies," *IEEE Commun. Surveys Tuts.*, vol. 21, no. 3, pp. 2568–2599, 3rd Quart., 2019.

[3]. I. Guvenc, C.-C. Chong, and F. Watanabe, "NLOS identification and mitigation for UWB localization systems," in *Proc. IEEE WCNC*, Hong Kong, 2007, pp. 1571–1576.

[4]. B. Denis, J. Keignart, and N. Daniele, "Impact of NLOS propagation upon ranging precision in UWB systems," in *Proc. IEEE Conf. UWB*, Nov. 2003, pp. 379–383.

[5]. Y. Cheng and T. Zhou, "UWB indoor positioning algorithm based on TDOA technology," in *Proc. ITME*, Aug. 2019, pp. 777–782.

[6]. F. Molisch, *Wireless Communications*, 2nd ed. Hoboken, NJ, USA: Wiley, 2011.

[7]. H. Wymeersch, S. Marano, W. M. Gifford, and M. Z. Win, "A machine learning approach to ranging error mitigation for UWB localization," *IEEE Trans. Commun.*, vol. 60, no. 6, pp. 1719–1728, Jun. 2012.

[8]. Z. Zeng, S. Liu, and L. Wang, "NLOS identification for UWB-based indoor positioning using CIR," in *Proc. ICSPCS*, Dec. 2018, pp. 1–6.

[9]. C. Jiang, J. Shen, S. Chen, Y. Chen, D. Liu, and Y. Bo, "UWB NLOS/LOS classification using deep learning methods," *IEEE Commun. Lett.*, vol. 24, no. 10, pp. 2226–2230, Oct. 2020.

[10]. S. Sung, H. Kim, and J.-I. Jung, "Accurate indoor positioning for UWB-based personal devices using deep learning," *IEEE Access*, vol. 11, pp. 20095–20111, 2023.

[11]. D.-H. Kim, G.-R. Kwon, J.-Y. Pyun, and J.-W. Kim, "NLOS identification in UWB channel for indoor positioning," in *Proc. IEEE CCNC*, Jan. 2018, pp. 1–4.

[12]. K. Wen, K. Yu, and Y. Li, "NLOS identification and compensation for UWB ranging based on obstruction classification," in *Proc. EUSIPCO*, Aug. 2017, pp. 2704–2708.

[13]. Q. Tian, K. I. Wang, and Z. Salcic, "Human body shadowing effect on UWB-based ranging system for pedestrian tracking," *IEEE Trans. Instrum. Meas.*, vol. 68, no. 10, pp. 4028–4037, Oct. 2019.

[14]. S. Haykin, *Kalman Filtering and Neural Networks*. New York, NY, USA: Wiley, 2001.

[15]. R. E. Kalman, "A new approach to linear filtering and prediction problems," *J. Basic Eng.*, vol. 82, no. 1, pp. 35–45, Mar. 1960.

[16]. S. Hochreiter and J. Schmidhuber, "Long short-term memory," *Neural Comput.*, vol. 9, no. 8, pp. 1735–1780, Nov. 1997.

[17]. A. Graves, A.-R. Mohamed, and G. Hinton, "Speech recognition with deep recurrent neural networks," in *Proc. IEEE ICASSP*, 2013, pp. 6645–6649.

[18]. Z. Xiao, H. Wen, A. Markham, and N. Trigoni, "Lightweight map matching for

International Research Journal on Advanced Engineering Hub (IRJAEH)
e ISSN: 2584-2137
Vol. 04 Issue: 02 February 2026
Page No: 604-612
https://irjaeh.com
https://doi.org/10.47392/IRJAEH.2026.0082

indoor localization using sequential models," *IEEE Trans. Mobile Comput.*, vol. 18, no. 11, pp. 2655–2668, Nov. 2019.

[19]. L. Schmid, D. Salido-Monzu, and A. Wieser, "Accuracy assessment and learned error mitigation of UWB ToF ranging," in *Proc. IPIN*, Sep. 2019, pp. 1–8.

[20]. D. Coppens *et al.*, "An overview of UWB standards and organizations (IEEE 802.15.4z, FiRa): Interoperability aspects and future research directions," *IEEE Access*, vol. 10, pp. 70219–70241, 2022.